VIP C–H Activation

DOI: 10.1002/anie.201100907

Evidence for a Precursor Complex in C–H Hydrogen Atom Transfer Reactions Mediated by a Manganese(IV) Oxo Complex**

*Isaac Garcia-Bosch, Anna Company, Clyde W. Cady, Stenbjörn Styring, Wesley R. Browne, Xavi Ribas, and Miquel Costas**

Dedicated to Professor Joaquín Borrás

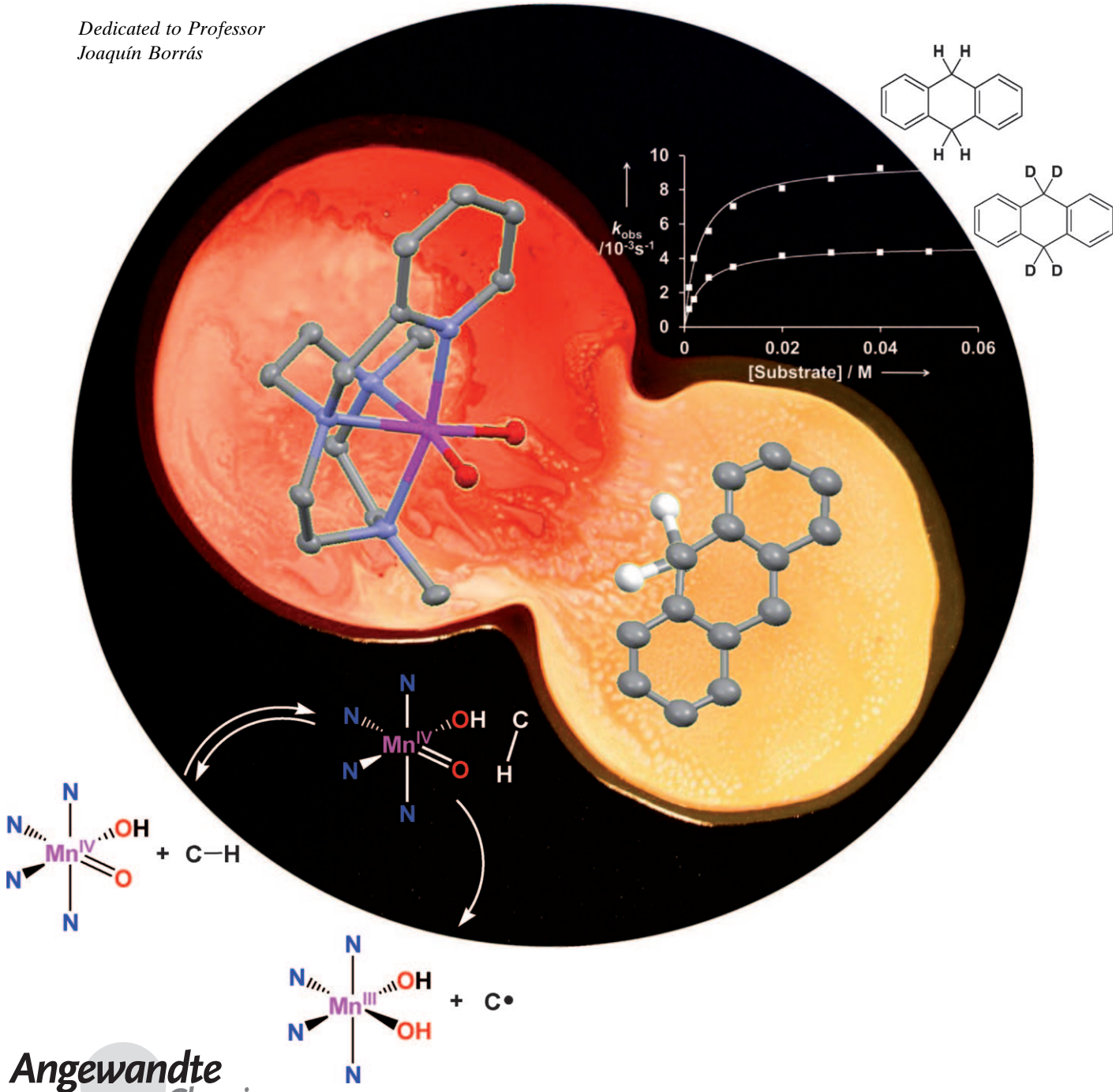

Hydrogen atom transfer (HAT) reactions mediated by transition-metal complexes are fundamental steps in many biological, environmental, and industrial chemical transformations.[1,2] Owing to their biological relevance, non-heme oxo iron(IV) compounds have been investigated intensively over the last years.[3,4] Manganese(V) oxo species and their role in C–H oxidation reactions have been also explored.[5] In contrast, the related mononuclear non-porphyrinic manganese(IV) oxo complexes remain elusive and their reactivity against C–H bonds has been seldom described.[6–10] Herein, we describe two novel non-porphyrinic mononuclear manganese(IV) bis(hydroxo) and manganese(IV) oxo(hydroxo) complexes and their ability to oxidize C–H bonds. We show that C–H oxidation by the Mn^{IV} oxo(hydroxo) species occurs by an unprecedented two-step reaction mechanism which involves a substrate–Mn^{IV}=O association event that precedes the C–H cleavage.

$[Mn^{IV}(OH)_2(^{H,Me}Pytacn)](CF_3SO_3)_2$ (**2**) was synthesized by oxidation of $[Mn^{II}(^{H,Me}Pytacn)](CF_3SO_3)_2$ (**1**)[11] with 10 equivalents of H_2O_2 in acetonitrile at 0 °C. X-Ray diffraction structural analysis[12] shows that the metal ion adopts a distorted octahedral geometry. Mn–O bond lengths and the stoichiometry of the compound provide a direct indication that **2** has two hydroxide ligands,[13] in a *cis* arrangement relative to each other (see Figure 1). Complex **2** is a rare example of a mononuclear Mn^{IV} complex with terminal hydroxide ligands, the only precedent is $[Mn^{IV}(OH)_2(Me_2EBC)](PF_6)_2$, which contains an ultrarigid, sterically demanding macrocyclic ligand.[13] Space-filling analysis (Figure 1) of **2** shows that one of the N-methyl groups, and the pyridine ring provide steric isolation of the metal center, and this is presumably the key structural feature to prevent the formation of the more common oligomeric species.

The conjugated base $[Mn^{IV}(O)(OH)(^{H,Me}Pytacn)]^+$ (**3**) was generated in situ in an acetonitrile/water mixture (5:1) by treating **2** with 1 equivalent of *t*BuOK. Titration with substoichiometric amounts of *t*BuOK was monitored by UV/Vis spectroscopy (Figure 2, top). The isosbestic point at λ_{max} = 652 nm demonstrates that the transformation occurs without the formation of additional long-lived intermediate species. This process is reversible, and **2** can be fully recovered by addition of 1 equivalent of CF_3SO_3H.

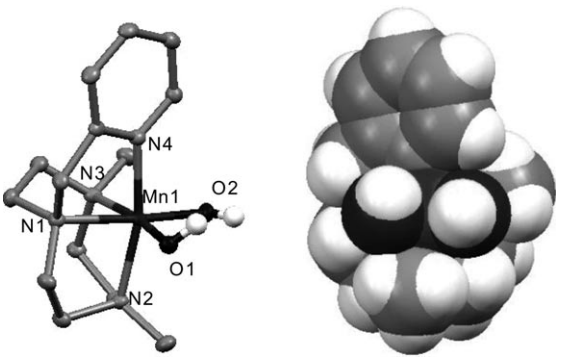

Figure 1. Thermal ellipsoid diagram (left), thermal ellipsoids set at 50% probability level, and space-filling diagram (right) of the cationic part of the crystal structure of $[Mn^{IV}(OH)_2(^{H,Me}Pytacn)](CF_3SO_3)_2$ (**2**). Selected bond lengths [Å]: Mn1-O1 1.805(2), Mn1-O2 1.793(2), Mn1-N1 2.057(3), Mn1-N2 2.043(2), Mn1-N3 2.106(3), Mn1-N4 2.003(3). For clarity, H atoms are omitted, except for those bound to O atoms.

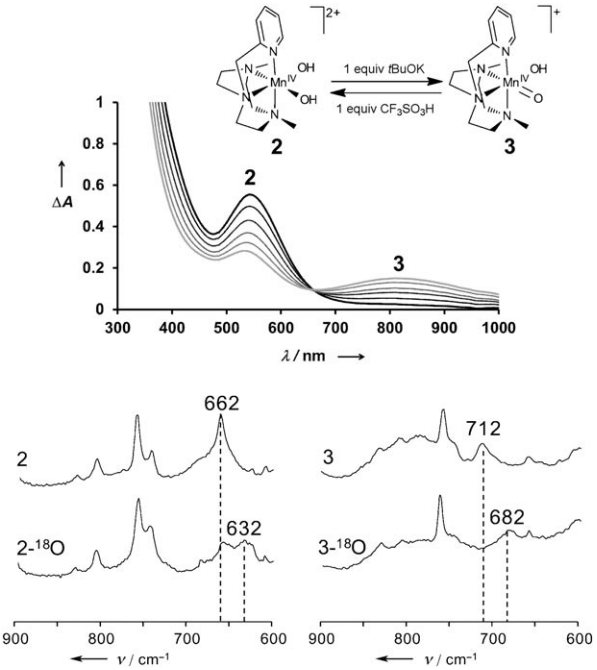

Figure 2. Top: UV/Vis spectra for the titration process from **2** to **3** (1 mM). Bottom: Raman spectra of complexes **2** and **3** in CH_3CN, and the corresponding complexes after addition of $H_2{}^{18}O$ (**2**-^{18}O and **3**-^{18}O).

ESI-MS spectra of **3** and **2** in CH_3CN solutions show signals for ions with *m*/*z* 336.1 and 168.5, with isotopic patterns consistent with $[Mn^{IV}(O)(OH)(^{H,Me}Pytacn)]^+$ and $[Mn^{IV}(OH)_2(^{H,Me}Pytacn)]^{2+}$, respectively. Addition of $H_2{}^{18}O$ to the initial solutions results in the disappearance of the original signals and emergence of new features at *m*/*z* 340.1 and 170.5, indicative of exchange with water and

[*] I. Garcia-Bosch, Dr. A. Company, Dr. X. Ribas, Dr. M. Costas
QBIS group, Departament de Química
Universitat de Girona
Campus de Montilivi, 17071 Girona, Catalonia (Spain)
E-mail: miquel.costas@udg.edu
Dr. C. W. Cady, Dr. S. Styring
Department of Photochemistry and Molecular Science
Uppsala University, Box 523, 75120 Uppsala (Sweden)
Dr. W. R. Browne
Stratingh Institute for Chemistry, University of Groningen
Nijenborgh 4, 9747 AG Groningen (The Netherlands)

[**] We thank Prof. Jim Mayer and Dr. Julio Lloret for reading this work and for helpful comments. M.C. thanks MICINN (CTQ2009-08464/BQU and PhD grants to I.G.-B) and the European Research Council (ERC-StG-239910). M.C. and X.R. acknowledge ICREA-Academia Awards, and SGR 2009-SGR637. S.S. thanks the Swedish Energy Agency, The K&A Wallenberg Foundation, and the EU/Energy project "SOLAR-H2". W.R.B. thanks Netherlands Technology Foundation STW grant no. 11059. RahuCat is acknowledged by a generous gift of tritosylTACN.

Supporting information for this article is available on the WWW under http://dx.doi.org/10.1002/anie.201100907.

formation of $[Mn^{IV}(^{18}O)(^{18}OH)(^{H,Me}Pytacn)]^+$ and $[Mn^{IV}(^{18}OH)_2(^{H,Me}Pytacn)]^{2+}$, respectively.

Vibrational data for both complexes was obtained by Raman spectroscopy (Figure 2, bottom). Complex **2** showed a Mn–O vibration at 662 cm^{-1} that shifted to 632 cm^{-1} in the presence of $H_2{}^{18}O$ ($\Delta\nu[^{18}O–^{16}O] = -30\ cm^{-1}$). These values are in close agreement with those reported for $[Mn^{IV}(OH)_2(Me_2EBC)](PF_6)_2$.[13] The Raman spectrum of complex **3** shows a new peak that appears at 712 cm^{-1} shifting to lower energies (682 cm^{-1}) in presence of $H_2{}^{18}O$ ($\Delta\nu[^{18}O–^{16}O] = -30\ cm^{-1}$). The energy of this feature is consistent with that of previously described Mn=O moieties.[8] In addition, the isotopic shift observed upon ^{18}O substitution is in agreement with that expected on the basis of Hooke's law for a Mn–O unit under the two-atom oscillator approximation.

The EPR spectrum of **2** is typical of mononuclear Mn^{IV} species (Supporting Information, Figure S5). The spectrum of a solution of **2** treated with one equivalent of *t*BuOK to form **3** shows a sharpening of the hyperfine structure observed in **2** (Supporting Information, Figure S5). This new signal is similar to other examples of Mn^{IV} signals.[14] The EPR assignment of both **2** and **3** as Mn^{IV} monomers is in good agreement with the solution-state effective magnetic moment for **2** and **3**, measured using the Evans' method at 298 K, which gives $\mu_{eff} = 4.09$ MB for **2**, and $\mu_{eff} = 3.99$ MB for **3**. Both values are close to the expected spin-only value for a $S = 3/2$ system.

The $E_{1/2}$ redox potentials of the Mn^{IV}/Mn^{III} couples associated with **2** and **3** were obtained from cyclic voltammetry (Supporting Information, Figure S6). For complex **2**, a reversible 1 e^- redox process at $E_{1/2} = 0.78$ V (versus the standard hydrogen electrode (SHE)) was observed. The corresponding $E_{1/2}$ redox potential for **3** could only be estimated from the anodic peak corresponding to the irreversible reduction to Mn^{III} ($E_{ap} = 0.4$ V approx.). The lack of reversibility arises from rapid protonation of the Mn^{III} oxo unit.

A $pK_a = 7.1 \pm 0.1$ was determined for the transformation of **2** to **3** by means of both spectrophotometric and potentiometric titrations (Supporting Information, Figure S7). This result is interesting because the related iron analogue $[Fe^{IV}(O)(OH_2)(^{H,Me}Pytacn)]^{2+}$ does not undergo protonation of the oxo ligand even at pH ≈ 1,[15] indicating that the corresponding $pK_a < 1$. These values show that in an analogous chemical environment, the Mn^{IV}=O unit is at least 7 p*K*a units more basic than Fe^{IV}=O.[16] By applying a Bordwell formalism,[17] both electrochemical and pK_a values can be used to calculate a bond dissociation energy $BDE_{3\text{-}H} = 83.4$ kcal mol^{-1} for the O–H bond in the complex $[Mn^{III}(OH)_2(^{H,Me}Pytacn)]^+$, (**3**-H), that is, the effect of adding a hydrogen atom to **3** (Supporting Information, Scheme S1). Unfortunately, the experimental data did not allow us to calculate the value for the complex $[Mn^{III}(OH)(OH_2)(^{H,Me}Pytacn)]^{2+}$, (**2**-H).

Complexes **2** and **3** were tested in the C–H oxidation of several substrates, including xanthene, 1,4-cyclohexadiene, 9,10-dihydroanthracene, and fluorene, in CH_3CN/H_2O 5:1 v/v (see Supporting Information for details). The oxidation state of the manganese after reaction with the substrates under N_2 was calculated by iodometric titration. The values of 3.3 ± 0.1 for complex **2** and 3.2 ± 0.2 for complex **3** indicate that both react as 1 e^- oxidants. When reactions are run under N_2, the corresponding product yields (Supporting Information, Table S1) account for (84 ± 10)% to (104 ± 10)% of the oxidizing equivalents. In contrast to **3**, complex **2** is not able to oxidize fluorene. As an illustrative example, the reaction of xanthene with **2** affords 9-xanthydrol as the major product (0.38 mmol/mmol **2**), and minor amounts of xanthone (0.06 mmol/mmol **2**) and 9,9′-bixanthyl (less than 0.01 mmol/mmol **2**; Scheme 1). Considering that these products formally correspond to 2 e^-, 4 e^-, and 2 e^- oxidation of xanthene, respectively, the electron balance accounts for (100 ± 6)% of the oxidizing equivalents. The presence of coupled products, such as 9,9′-bixanthyl and 9,9′-bifluorenyl in the oxidation of xanthenes and fluorene, respectively, are indicative of freely diffusing radicals.

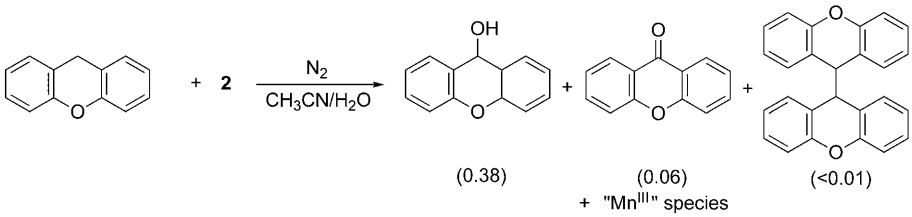

Scheme 1. Oxidation of xanthene with **2**. Indicated in parenthesis are the mol product/mol **2** produced.

To elucidate mechanistic details of the C–H bond cleavage reaction, kinetic analysis was conducted on the reaction of **2** and **3** with the substrates (Table 1). Reactions were monitored by UV/Vis spectroscopy, tracking the decay of the manganese(IV) species at $\lambda = 545$ nm for **2** and $\lambda = 825$ nm for **3** (see Supporting Information for full details on the kinetic analysis). Reactions of **2** can be analyzed as bimolecular processes, with a first-order dependence both in substrate and complex concentrations. A plot of $\log(k_2^{(OH)})$ ($k_2^{(OH)}$ = second-order rate constant) against substrate C–H BDEs[18] (Table 1) showed a linear dependence with a slope of 0.36. Kinetic isotope effects (KIE) values obtained from the oxidation reaction rate of $[D_2]$xanthene, and $[D_4]$1,4-cyclohexadiene are 8.0, and 6.6, respectively. These large values indicate that C–H bond cleavage occurs at the rate-determining step (r.d.s.) of the reaction. The sum of all these observations provides strong evidence that reactions performed by **2** proceed by abstraction of a hydrogen atom (a HAT reaction) by the $Mn^{IV}(OH)_2$ unit (Figure 3).[1,2]

In contrast with that found for complex **2**, complex **3** has a completely different kinetic behavior in its reaction with C–H bonds. Saturation plots were obtained when the concentration of substrate was increased (Figure 3, bottom). The simplest model to account for this scenario is the presence of a

Table 1: BDE_{C-H} values, pK_a values, redox potentials, and rate constants for the reaction of **2** and **3** with various substrates at 298 K.

Substrate	BDE_{C-H} [kcal mol^{-1}][a]	pK_a[a]	E_{ox}[a,b]	**2** $k_2^{(OH)}$ [10^{-4} M^{-1} s^{-1}]	**2** K_{eq} [M^{-1}]	**3** $k_2^{(O)}$ [10^{-4} s^{-1}]	**3** $K_{eq}k_2^{(O)}$ [M^{-1} s^{-1}]
xanthene	75.5	30	−1.685	116 ± 4	317 ± 20	97 ± 4	3.07
[D_2]xanthene	–	–	–	15 ± 2	273 ± 15	48 ± 2	1.31
1,4-cyclohexadiene	77	–	–	50 ± 2	250 ± 10	78 ± 5	1.95
9,10-dihydroanthracene	78	30.1	−1.575	16 ± 1	523 ± 33	65 ± 4	3.40
[D_4]9,10-dihydroanthracene	–	–	–	5.6 ± 1	493 ± 28	21 ± 1	1.04
fluorene	80	22.6	−1.069	–	363 ± 10	18 ± 1	0.65

[a] For BDE_{C-H}, pK_a, and E_{ox} values see Ref. [17,18]. [b] E_{ox} referred to irreversible oxidation potentials of the corresponding anions [kcal mol^{-1}].

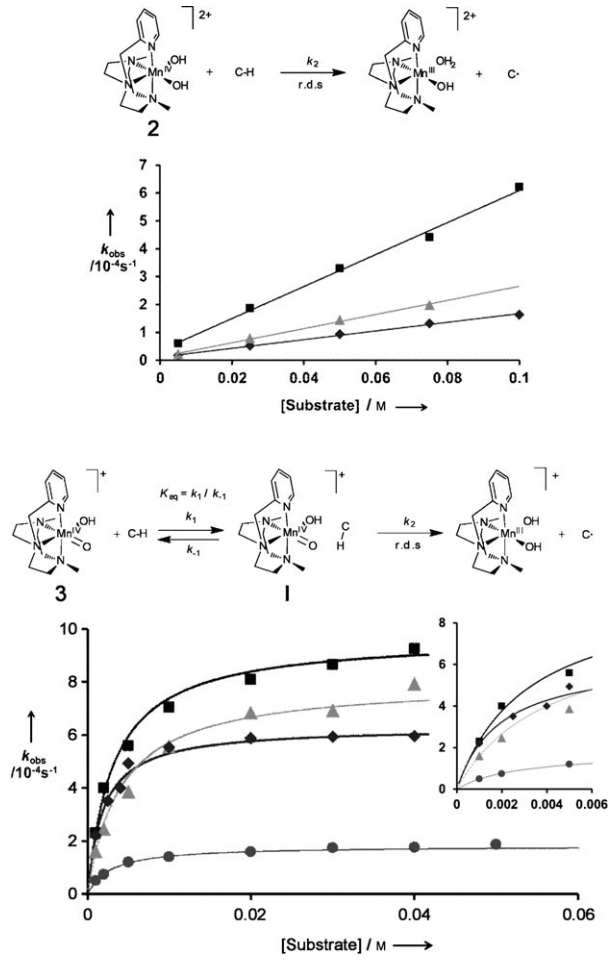

Figure 3. Reaction of complex **2** (top) and complex **3** (bottom) with different substrates (xanthene = ■, 1,4-cyclohexadiene = ▲, 9,10-dihydroanthracene = ◆, fluorene = ●). Inset in bottom plot: expansion of the low [substrate] region.

relatively fast equilibrium that precedes the rate-determining step. Accordingly, the data can be satisfactorily fitted by the equation $k_{obs} = k_2^{(O)}K_{eq}[substrate]/(1+K_{eq}[substrate])$ were K_{eq} is the equilibrium constant and $k_2^{(O)}$ is the first-order rate constant of the rate-determining step.[19] Consistent with the involvement of the substrate in the pre-equilibrium event (Table 1) both K_{eq} and $k_2^{(O)}$ values are dependent on the substrate: while $\log(k_2^{(O)})$ values decrease linearly when the BDE_{C-H} increases, the equilibrium constant K_{eq} does not show a direct relation with the BDE_{C-H}. The latter observation is compatible with a HAT in the rate-determining step, and not during the pre-equilibrium. Furthermore, the K_{eq} values do not correlate either with pK_a or $E_{1/2}$ values for a 1 e$^-$ oxidation of the substrate. Indeed, these values indicate that proton transfer (PT) and electron transfer (ET) from xanthene, 9,10-dihydroanthracene, and fluorene to **3** can be discounted because they are highly endergonic reactions. KIE experiments provide strong evidence that C–H breakage occurs in the second reaction. The equilibrium constants K_{eq} show little dependence on deuteration ($K_{eq(xanthene)}/K_{eq([D_2]xanthene)} = 1.2$, $K_{eq(9,10\text{-dihydroanthracene})}/K_{eq([D_4]9,10\text{-dihydroanthracene})} = 1.1$). However, $k_2^{(O)}$ for both [D_2]xanthene and [D_4]9,10-dihydroanthracene has values consistent with a primary KIE of 2.0 and 3.1, respectively. Thus, the kinetic data indicates that a reversible associative process between substrate and the oxo manganese(IV) complex **3** takes place, forming an intermediate species **I**, and that C–H cleavage occurs, most likely by a HAT, during the second reaction step.

Insight into the nature of **I** could be obtained by UV/Vis spectroscopy. Monitoring of the reactions under saturation conditions at short reaction times shows small alterations in the energy ($\Delta\lambda_{max} < 4$ nm) of the visible spectral features of **3**. K_{eq} constants indicate that under these conditions, **I** should be the major species in solution. The lack of major differences in its UV/Vis spectrum with respect to that of **3** is a strong indication that both oxidation state and coordination characteristics of the Mn ion are preserved. We therefore suggest that **I** results from weak non-covalent interactions; although the nature of species **I** is unclear, a hydrogen-bond interaction between the rather basic oxo ligand and the substrate C–H bond is likely to be involved.[20,21]

From a van't Hoff plot the thermodynamic parameters of the equilibrium step relating **3**, 9,10-dihydroanthracene, and **I** were calculated as $\Delta H° = (-3.6 \pm 0.2)$ kcal mol^{-1} and $\Delta S° = (0.3 \pm 0.4)$ cal K^{-1} mol^{-1} ($\Delta G° = (-3.7 \pm 0.2)$ kcal mol^{-1} (298 K)). As expected, the reaction is exothermic and it is enthalpically driven. The low $\Delta S°$ value is somewhat surprising for an associative reaction and likely indicates that it involves desolvation of at least one of the two reagents.

Temperature-dependent kinetic analyses of the HAT reactions (k_2) were performed using 9,10-dihydroanthracene as substrate (See Supporting Information). The Eyring plots provide activation parameters for **2** ($\Delta H^{\neq} = (6.6 \pm 0.1)$ kcal mol^{-1}, $\Delta S^{\neq} = (-51.9 \pm 0.3)$ cal K^{-1} mol^{-1}) and for the precursor complex **I** ($\Delta H^{\neq} = (10.3 \pm 0.7)$ kcal mol^{-1}, $\Delta S^{\neq} = (-37 \pm 2)$ cal K^{-1} mol^{-1}). The difference in the $\Delta H^{\neq}$ should reflect the difference between the BDE_{OH} of **2**-H and **I**. The negative

$\Delta S^{\neq}$ value for **2** is consistent with the bimolecular nature of the rate-determining step. In the case of the encounter species **I**, the negative $\Delta S^{\neq}$ value is indicative of a more organized transition state, ready for the hydrogen atom transfer rate-determining step.

Mayer et al. have developed a conceptual framework for HAT reactions based on the Marcus theory for electron transfer (ET) reactions.[22] As in Marcus theory, HAT reactions are proposed to occur by formation of an initial H-donor/H-acceptor precursor or encounter complex, which then undergoes a proton-coupled electron transfer (PCET) to form a successor complex that then dissociates. The nature of the precursor complex in HAT could be quite different from that of ET. Electrons can tunnel over multiple-Ångstrom distances, and because of that, very specific donor–acceptor orientations are not strictly required for ET. In contrast the transfer of a H nuclei in HAT reactions occurs over very short distances, along very specific axes and usually within a hydrogen bond. Experimental identification of a precursor complex in HAT reactions has only been accomplished in two recent examples, and in both cases the substrate contains an OH unit that can engage in hydrogen-bond interactions with the hydrogen abstracting agent.[23,24] Precursor species observed in HAT reactions mediated by **3** are thus unprecedented.

Several interesting conclusions are derived from the kinetic analysis and the mechanistic scenario that emerges therein; from inspection of the reaction rates of **2** ($k_2^{(OH)}$) and **3** ($K_{eq}k_2^{(O)}$) (Table 1), we conclude that in general the terminal oxo ligand in **3** appears to be a better H-abstraction agent than the hydroxide ligand in **2**. The higher basicity of the terminal oxo in comparison with the hydroxide ligand is commonly understood as the reason for this relative reactivity.[7,9,25]

Analysis of the kinetic parameters associated with the oxidation of 9,10-dihydroanthracene indicates that **I** has a kinetic preference (smaller $\Delta G^{\neq}$ value) over **2**. This preference has an entropic ($\Delta\Delta S^{\neq} = 14.9\ \text{cal}\,\text{K}^{-1}\,\text{mol}^{-1}$) but not an enthalpic ($\Delta\Delta H^{\neq} = 3.7\ \text{kcal}\,\text{mol}^{-1}$) origin. The entropic disadvantage of **2** is expected because of the bimolecular nature of its HAT reactions, while **I** reacts in a unimolecular process. However, the enthalpic preference of **2** is unexpected, given the overall higher reactivity of **3** with respect to **2**. We infer that in the encounter complex **I**, the basicity of the oxo ligand is attenuated by the hydrogen bonding. In addition, the thermodynamic characteristics of the equilibrium that describes the formation of the precursor significantly affect the overall reaction rate (k_{obs}) by which **3** reacts with a C–H bond, and consequently also determine the relative reactivity of **3** to C–H bonds with respect to that of **2**. Last, and probably most surprising, despite that the overall reaction between **3** and a particular C–H bond is a HAT, relative reaction rates among different substrates, commonly dictated by substrate C–H BDEs, can be altered. Since $k_{obs} = k_2^{(O)}K_{eq}[\text{substrate}]/(1+K_{eq}[\text{substrate}])$, both the K_{eq} (thermodynamics of the equilibrium leading to precursor **I** formation), and substrate concentration influence the relative reactivity of **3** to the point that stronger C–H bonds may react faster than weaker C–H bonds. In fact, this situation is reflected in Figure 3, where 9,10-dihydroanthracene ($BDE_{C-H} = 78\ \text{kcal}\,\text{mol}^{-1}$), which has the highest equilibrium constant ($K_{eq} = 523\ \text{M}^{-1}$) reacts at faster reaction rates (k_{obs}) than xanthene and 1,4-cyclohexadiene at low substrate concentrations, where the equilibrium control is expected and has a major impact in the observed rates. At higher substrate concentrations, relative reaction rates then become dominated by $k_2^{(O)}$, that is, by the C–H BDE.

In conclusion, we have synthesized and characterized two new mononuclear non-porphyrinic manganese(IV) complexes with hydroxide and oxide ligands, and studied their reactivity in C–H bond HAT reactions. Reactions of oxo manganese complex **3** provide the first experimental evidence for the involvement of a C–H substrate/H-abstractor encounter complex **I** in a C–H bond HAT reaction. Formation of such encounter complexes has been postulated within the framework of the formal analogies between HAT and electron transfer (ET) reactions.[22] Most interestingly, the thermochemical parameters associated with the formation of this precursor complex affect not only the overall C–H oxidation rate but can also alter the relative C–H reactivity in HAT. Hence it does not follow the trend expected on the basis of C–H BDEs. These observations expand our understanding on the mechanisms of C–H oxidation by metal oxo species.

Received: February 4, 2011
Published online: April 14, 2011

Keywords: C–H activation · hydrogen atom transfer · kinetics · manganese · metal oxo compounds

[1] J. J. Warren, T. A. Tronic, J. M. Mayer, *Chem. Rev.* **2010**, *110*, 6961 – 7001.
[2] M. H. V. Huynh, T. J. Meyer, *Chem. Rev.* **2007**, *107*, 5004 – 5064.
[3] J. Kaizer, E. J. Klinker, N. Y. Oh, J.-U. Rohde, W. J. Song, A. Stubna, J. Kim, E. Munck, W. Nam, L. Que, Jr., *J. Am. Chem. Soc.* **2004**, *126*, 472 – 473.
[4] C. V. Sastri, J. Lee, K. Oh, Y. J. Lee, J. Lee, T. A. Jackson, K. Ray, H. Hirao, W. Shin, J. A. Halfen, L. Que, Jr., S. Shaik, W. Nam, *Proc. Natl. Acad. Sci. USA* **2007**, *104*, 19181 – 19186.
[5] a) J. T. Groves, J. Lee, S. S. Marla, *J. Am. Chem. Soc.* **1997**, *119*, 6269 – 6273; b) W. J. Song, M. S. Seo, S. D. George, T. Ohta, R. Song, M.-J. Kang, T. Tosha, T. Kitagawa, E. I. Solomon, W. Nam, *J. Am. Chem. Soc.* **2007**, *129*, 1268 – 1277; c) K. A. Prokop, S. P. de Visser, D. P. Goldberg, *Angew. Chem.* **2010**, *122*, 5217 – 5221; *Angew. Chem. Int. Ed.* **2010**, *49*, 5091 – 5295.
[6] T. H. Parsell, R. K. Behan, M. T. Green, M. P. Hendrich, A. S. Borovik, *J. Am. Chem. Soc.* **2006**, *128*, 8728 – 8729.
[7] a) G. Yin, A. M. Danby, D. Kitko, J. D. Carter, W. M. Scheper, D. H. Busch, *J. Am. Chem. Soc.* **2008**, *130*, 16245 – 16253; b) S. Chattopadhyay, R. A. Geiger, G. Yin, D. H. Busch, T. A. Jackson, *Inorg. Chem.* **2010**, *49*, 7530 – 7535.
[8] S. C. Sawant, X. Wu, J. Cho, K.-B. Cho, S. H. Kim, M. S. Seo, Y.-M. Lee, M. Kubo, T. Ogura, S. Shaik, W. Nam, *Angew. Chem.* **2010**, *122*, 8366 – 8370; *Angew. Chem. Int. Ed.* **2010**, *49*, 8190 – 8194.
[9] T. H. Parsell, M.-Y. Yang, A. S. Borovik, *J. Am. Chem. Soc.* **2009**, *131*, 2762 – 2763.
[10] T. Kurahashi, A. Kikuchi, Y. Shiro, M. Hada, H. Fujii, *Inorg. Chem.* **2010**, *49*, 6664 – 6672.
[11] I. Garcia-Bosch, A. Company, X. Fontrodona, X. Ribas, M. Costas, *Org. Lett.* **2008**, *10*, 2095 – 2098.

[12] CCDC 811699 (**2**) contains the supplementary crystallographic data for this paper. These data can be obtained free of charge from The Cambridge Crystallographic Data Centre via www.ccdc.cam.ac.uk/data_request/cif.
[13] G. Yin, J. M. McCormick, M. Buchalova, A. M. Danby, K. Rodgers, V. W. Day, K. Smith, C. M. Perkins, D. Kitko, J. D. Carter, W. M. Scheper, D. H. Busch, *Inorg. Chem.* **2006**, *45*, 8052 – 8061.
[14] T. M. Rajendiran, J. W. Kampf, V. L. Pecoraro, *Inorg. Chim. Acta* **2002**, *339*, 497 – 502.
[15] A. Company, I. Prat, J. Frisch, R. Mas-Ballesté, M. Güell, G. Juhász, X. Ribas, E. Münck, J. M. Luis, L. Que, Jr., M. Costas, *Chem. Eur. J.* **2011**, *17*, 1622 – 1634.
[16] For a related comparison between Fe^{III} and Mn^{III} species, see: a) C. R. Goldsmith, A. P. Cole, T. D. P. Stack, *J. Am. Chem. Soc.* **2005**, *127*, 9904 – 9912; b) C. R. Goldsmith, R. T. Jonas, T. D. P. Stack, *J. Am. Chem. Soc.* **2002**, *124*, 83 – 96.
[17] F. G. Bordwell, J. P. Cheng, J. A. Harrelson, *J. Am. Chem. Soc.* **1988**, *110*, 1229 – 1231.
[18] Y.-R. Luo, *Comprehensive Handbook of Chemical Bond Energies*, CRC, Boca Raton, **2007**.
[19] Saturation curves could also be fitted by assuming a substrate-independent pre-equilibrium ($K_{eq} = k_1/k_{-1}$) and a subsequent bimolecular reaction with the substrate (k_2[substrate]). However, K_{eq} values will need to be substrate independent, and reaction rates for all substrates will need to overlay at saturation conditions ($k_{obs} = k_1$). Because of that, this scenario is disregarded.
[20] T. Steiner, *Angew. Chem.* **2002**, *114*, 50 – 80; *Angew. Chem. Int. Ed.* **2002**, *41*, 48 – 76.
[21] Elucidation of the molecular nature of **I**, and the possible role of the solvent, especially water molecules, are currently underway.
[22] J. M. Mayer, *Acc. Chem. Res.* **2011**, *44*, 36 – 46.
[23] T. Kojima, Y. Hirai, T. Ishizuka, Y. Shiota, K. Yoshizawa, K. Ikemura, T. Ogura, S. Fukuzumi, *Angew. Chem.* **2010**, *122*, 8627 – 8631; *Angew. Chem. Int. Ed.* **2010**, *49*, 8449 – 8453.
[24] E. A. Mader, J. M. Mayer, *Inorg. Chem.* **2010**, *49*, 3685 – 3687.
[25] M. T. Green, J. H. Dawson, H. B. Gray, *Science* **2004**, *304*, 1653 – 1656.

